Macroalgae contribute to nested mosaics of pH variability in a sub-Arctic fjord

D. Krause-Jensen*[1,2], C. M. Duarte[3,4], I. E. Hendriks[5], L. Meire[6,7,8], M. E. Blicher[6], N. Marbà[5], M. K. Sejr[1,2]

[1]Arctic Research Centre, Bioscience, Aarhus University, C.F. Møllers Allé 8, 8000 Århus C, Denmark

[2]Department of Bioscience, Aarhus University, Vejlsøvej 25, 8600 Silkeborg, Denmark

[3] Red Sea Research Center, King Abdullah University of Science and Technology, Thuwal 23955-6900, Kingdom of Saudi Arabia

[4] Faculty of Biosciences, Fisheries and Economics, University of Tromsø, Tromsø, Norway

[5]Department of Global Change Research, IMEDEA (CSIC-UIB) Instituto Mediterráneo de Estudios Avanzados, Miquel Marqués 21, 07190 Esporles, Spain

[6]Greenland Climate Research Centre, Greenland Institute of Natural Resources, Kivioq 2, Box 570, 3900 Nuuk, Greenland

[7]Marine Biology Laboratory, University of Ghent (UGent), Krijgslaan 281 (S8), 9000 Gent, Belgium

[8]Royal Netherlands Institute of Sea Research (NIOZ), Department of Ecosystem Studies, Korringaweg 7, 4401 NT, Yerseke, The Netherlands

*Correspondance e-mail: dkj@bios.au.dk

Abstract. The Arctic Ocean is considered the most vulnerable ecosystem to ocean acidification and large-scale assessments of pH and the saturation state for aragonite (Ω_{arag}) have let to the notion that the Arctic Ocean is already close to corrosive states. In high-latitude coastal waters the regulation of pH and Ω_{arag} is, however, far more complex than offshore because increased biological activity and input of glacial meltwater affect pH. Effects of ocean acidification on calcifiers and non-calcifying phototrophs occupying coastal habitats cannot be derived from extrapolation of current and forecasted offshore conditions, but requires an understanding of the regimes of pH and Ω_{arag} in their coastal habitats. To increase knowledge of the natural variability of pH in the Arctic coastal zone and specifically to test the influence of benthic vegetated habitats, we quantified pH-variability in a Greenland fjord in a nested scale approach. A sensor array logging pH, O_2, PAR, temperature and salinity was applied on spatial scales ranging from km-scale across the horizontal extension of the fjord, over 100 m-scale vertically in the fjord, 10-100 m scale between subtidal habitats with and without kelp forests and between vegetated tidal pools and adjacent vegetated shores, to cm-m scale within kelp forests and mm-scale across diffusive boundary layers of macrophyte tissue. In addition, we assessed the temporal variability in pH on diurnal and seasonal scales. Based on pH-measurements combined with point samples of total alkalinity, dissolved inorganic carbon and relationships to salinity, we also estimated variability of Ω_{arag}. Results show variability in pH and Ω_{arag} of up to 0.2-0.3 units at several scales, i.e. along the horizontal and vertical extension of the fjord, between seasons and on a diel basis in benthic habitats and within $1m^3$ of kelp forest. Vegetated intertidal pools exhibited extreme diel pH variability of >1.5 units and macrophyte diffusive boundary layers a pH range of up to 0.8 units. Overall, pelagic and benthic metabolism was an important driver of pH and Ω_{arag} producing mosaics of variability from low levels in the dark to peak levels at high irradiance generally appearing favorable for calcification. We suggest that productive coastal environments may form niches of high pH in a future acidified Arctic

Ocean.

1. Introduction

The Arctic Ocean is considered to be the most vulnerable ecosystem to ocean acidification due to the combined effects of low temperature, which increases the solubility of CO_2 and, at places, dilution of the buffering capacity of seawater by freshwater inputs (Fabry et al., 2009, AMAP, 2013). Indeed, large-scale assessments of pH in combination with saturation states for aragonite (Ω_{arag}) < 1 have led to the notion that the Arctic Ocean is already in close proximity to corrosive state (Fabry et al., 2009). However, whereas this has been documented for offshore waters, the Arctic contains a massive coastline where the regulation of pH and Ω_{arag} is far more complex than that offshore (Hofmann et al. 2011, Duarte et al., 2013). In coastal waters, the role of air-sea CO_2 exchange in regulating pH operates along with watershed effects driven by the discharge of freshwater and the effects of metabolically intense communities on pH (Duarte et al. 2013). The Greenland Ice Sheet is melting at a rate that has more than doubled in the recent decade (Helm et al. 2014) and Greenland fjords are, hence, potentially among the most susceptible to the effects of freshening and acidification.

As most calcifiers occupy coastal habitats, the assessment of risks of Arctic acidification to these vulnerable species cannot be derived from extrapolation of the current and forecasted offshore conditions alone, but requires an understanding of the regimes of pH and Ω_{arag} in the coastal habitats they occupy, and the same is true regarding potential effects of ocean acidification on coastal phototrophs (calcifying or non-calcifying) (Mercado and Gordillo, 2011). Such information is currently largely lacking for the Arctic in general and for Greenland in particular, which calls for efforts to understand variability of pH in the coastal zone informing on the factors controlling pH

and ultimately determining the sensitivity of the coastal Arctic Ocean ecosystem to ocean acidification.

Greenland has a vast and highly indented coastline, extending approximately 44,000 km and representing ca. 12% of the world's coastline (Krause-Jensen and Duarte, 2014). This coastline forms a complex network of fjords and open coasts that contains multiple features contributing to heterogeneity, such as continental ice and freshwater discharge at the headwaters, variable slopes and substrates, differential water residence time conducive to widely distinct temperature regimes within neighboring areas (Olesen et al., 2015), and tides that generate intertidal habitats and force flow patterns. In addition, Greenland fjords often support highly productive kelp forests (Krause-Jensen et al., 2012) and intertidal seaweed communities (Høgslund et al., 2014), which have been suggested to have the capacity to affect pH and Ω_{arag} locally (Krause-Jensen and Duarte, 2014). Such effects have been demonstrated for Antarctic and temperate kelp/macroalgal ecosystems (Middelboe & Hansen 2007, Delille et al. 2009, Cornwall et al. 2013a) as well as for subtropical and tropical seagrass meadows (e.g. Hofmann et al. 2011, Hendriks et al. 2014). Calcifiers such as bivalves, brittle stars and sea urchins, which are potentially vulnerable to OA, are ecologically important as they contribute significantly to carbon cycling in both sub-Arctic and Arctic Greenland where their distribution range from the intertidal zone to >300 m depth (Sejr et al., 2002; Blicher et al., 2007, 2009, 2013 Blicher and Sejr, 2011). Phototrophs such as kelps, while being able to affect the pH regime, may also respond to OA, which has been shown to stimulate their growth (Olischläger et al. 2012) and affect the competition between kelps and understory red algae (Connell and Russell 2010).

Although the variability in pH and Ω_{arag} in Greenland fjords has not been reported, available oceanography and environmental surveys suggest that this may be substantial. For instance, in Young Sound, Sejr et al. (2011) found that the extent of sea-ice cover and inputs of glacial melt water affect seawater pCO_2 levels and sea-air exchange at spatial, seasonal and inter-annual scales. Seasonal dynamics of autotrophic and heterotrophic plankton metabolism have also been found to markedly affect pCO_2 levels in Kobbefjord, a sub-Arctic fjord in SW Greenland (Sejr et al., 2014). However, information on scales of variability in pH and Ω_{arag} in Greenland fjords is still lacking, precluding the assessment of their current and future vulnerability to ocean acidification.

Here we quantify pH variability in Kobbefjord, SW Greenland. This sub-Arctic fjord supports dense and productive subtidal kelp forests, intertidal macroalgal habitats and high abundance of bivalves and sea urchins with important roles in the ecosystem (Blicher et al. 2009; Krause-Jensen et al., 2012). We hypothesize that Kobbefjord contains a mosaic of pH environments nested across a range of scales of variability and that primary production in general, and by macroalgae in particular, may be an important driver of pH variability relevant for benthic calcifiers. We first assess seasonal and spatial variability in the open water pH at km scale along the horizontal extension and at 100 meter scale vertically in the fjord. We then examine diel variability in pH within subtidal benthic habitats colonized by kelp forest or microalgae/scattered filamentous algae as well as in vegetated tidal pools and adjacent vegetated intertidal shores, with the distance between parallel deployments at the 10-100 m scale. We further explore the pH variability 3-dimensionally at cm- to m-scale within the kelp forest ecosystem and at mm-scale across the diffusive boundary layer (i.e. the layer in which molecular diffusion is the dominant transport mechanism for dissolved material, see e.g. de Beer and Larkum 2001) of key macrophyte species. Whereas our assessment focuses on pH, we also discuss the associated variability of Ω_{arag}.

2. Methods

2.1. Study area

Kobbefjord is located in the extensive Godthåbsfjord system in south west Greenland (Fig. 1A). The fjord is 17 km long and 0.8–2 km wide and has a maximum depth of 150 m. It is subjected to marked exchange of coastal water driven by a tidal range of 1- 4.5 m (Richter et al. 2011) and receives freshwater mainly from a river in the innermost part of the fjord, leading to a salinity gradient in the surface water. Sea-ice usually covers the inner part of the fjord from December to early May, but the outer part of the fjord is permanently ice free. Light attenuation in the water column has been reported to range from 0.083 m^{-1} in February over 0.197 m^{-1} in May to 0.135 m^{-1} in September (Sejr et al. 2014). Whereas the phytoplankton community is the main primary producer in the central parts of the fjord (Sejr et al., 2014), subtidal macroalgae, dominated by *Saccharina longicruris* and *Agarum clathratum* form productive benthic habitats along the shores to water depths of ca. 40 m (Krause-Jensen et al., 2012) interspaced with communities of benthic microalgae (Glud et al., 2010, Attard et al. 2014) as well as with scattered eelgrass (*Zostera marina*) meadows at 1-3 m depth (Olesen et al., 2015). Communities of intertidal macroalgae, dominated by *Fucus* spp. and *Ascophyllum nodosum* are prominent in the intertidal zone where they form an important habitat for e.g. blue mussel (Blicher et al., 2013).

Three field campaigns targeting seasonal- and fjord-scale variability in pH in the pelagic zone were conducted in the spring (19 April), mid-summer (18 July) and late summer (3 September) of 2013 (Fig. 1B). The late summer survey was associated with an intensive campaign (27 August- 6 September 2013) exploring pH variability in shallow subtidal kelp habitats and neighboring habitats colonized by benthic microalgae and scattered filamentous algae (Fig. 1C). A final late summer

campaign (22-30 August 2014) addressed pH variability in vegetated tidal pools and surface waters of adjacent vegetated shores (Fig. 1C). All pH data from fjord-scale to micro-scale are reported on the total pH scale.

2.2. Fjord and seasonal scale pH variation

To determine the large-scale spatial and seasonal variation in physical and chemical parameters in the water column of Kobbefjord, vertical profiles were performed at 11 stations located along a longitudinal gradient following the main central axis of the fjord on 19 April, 18 July, and 3 September, 2013 (Fig. 1B). We used a Seabird CTD (SBE19plus) equipped with sensors for temperature, conductivity, fluorescence (Seapoint Chlorophyll Fluorometer), oxygen (SBE 43, Seabird) and pH (SBE18, Seabird). Alongside CTD profiles, water samples were collected using a 5 L Niskin bottle at 1, 5, 10, 20, 30, and 40 m depth. Water was collected for dissolved oxygen measurement using Winkler titration (Parsons et al. 1984), which was used to calibrate the CTD oxygen optode. The pH sensor was calibrated using NIST buffers and a seawater TRIS buffer prepared according to Dickson (2007). Unfiltered water was transferred to 150 ml borosilicate glass bottles for pH analysis. The samples were poisoned with a saturated mercuric chloride solution, cooled and stored in darkness until arrival. Back in the lab, pH was measured potentiometrically using a glass reference electrode (Orion, Ross Ultra pH/ATC Triode) calibrated with NIST buffers and a seawater TRIS buffer prepared according to Dickson (2007). The measurements were used to correct the offset of the SBE 18 pH measurements.

For estimation of the saturation state of aragonite (Ω_{arag}), samples for analyses of dissolved inorganic carbon (C_T) and total alkalinity (A_T) were collected at 5 stations on one occasion (3 September 2013). Triplicate 12 ml samples were collected at 5, 10, 20, 30, and 40 m depth and near

167 the bottom. Samples were carefully siphoned through tygon tubing from Niskin bottles to 12 ml
168 septum-capped glass vial (exetainers) allowing the water to overflow for two volume changes. The
169 samples were poisoned with 100 µl 5% $HgCl_2$ to avoid biological alteration. C_T was analyzed with
170 a C_T analyzer (AS-C3, Apollo Scitech Inc). The accuracy of the analysis was 2.4 µmol kg^{-1}
171 (average numerical deviation from the reference material value) and the precision was 1.4 µmol kg^{-}
172 ^{1} (average standard deviation of triplicate samples). A_T was analysed on an alkalinity titrator, AS-
173 ALK2 from Apollo Scitech with verification against the same certified reference material used for
174 pH measurements or a Metrohm Titrando 808 by open cell titration (Dickson et al. 2007) using
175 Batch 136 supplied by the Andrew Dickson lab at UC San Diego for verification. Average analysis
176 accuracy was 2.9 µmol kg^{-1} (average numerical deviation from the reference material value).
177 Relationships between the point samples of A_T and salinity (S) were used to verify the published
178 relationship for the Godthåbsfjord system (TA=159+63S, Meire et al. 2015) which was
179 subsequently applied for estimation of A_T for the full September data set. Ω_{arag} and *p*CO2 were
180 calculated from A_T and pH using the CO_2SYS excel programme version 2.1 (Pierrot et al., 2006)
181 with the K_1 and K_2 constants from Mehrbach et al. (1973), as modified by Dickson and Millero
182 (1987).
183
184 *2.3. Small-scale and diurnal-scale pH variation*
185 To measure small-scale and diurnal-scale variation in pH and physico-chemical variables in kelp
186 forests and adjacent sub-tidal habitats colonized by microalgae and scattered filamentous algae we
187 constructed metal frames measuring approximately 0.90 m × 0.90 m × 1.10 m. Each frame was
188 equipped with instruments that allowed continuous measurements of temperature, salinity, water
189 level, oxygen concentration, photosynthetically active radiation (PAR) and pH at ca 50 cm above
190 the seafloor (Fig. 1S). Measurements were made every 10 min or less. - We selected three dense

191 (close to 100% cover) kelp beds located in shallow water (average depth 2-5 m) in different sites of
192 the fjord. All kelp beds were dominated by *S. longicruris* with co-occurrence of *A. clathratum* and
193 were surrounded by habitats colonized by microalgae and varying amounts of scattered filamentous
194 algae. We conducted parallel deployments of frames with loggers in kelp beds vs. surrounding non-
195 kelp habitats in each of the three sites, with each deployment lasting about 48 h. The typical
196 distance between kelp and non-kelp habitats at each site was approximately 100 m. Conductivity,
197 temperature and water level were measured by Hydrolab DS5X and MicroCat (SBE37 Seabird).
198 Oxygen concentration was measured using MiniDot oxygen loggers, Precision Measurement
199 Engineering, and Hydrolab DS5X. PAR was measured using Odyssey PAR loggers from Dataflow
200 Systems Pty Limited. pH was measured using Hydrolab DS5X and SeaFET pH loggers from
201 Satlantic. Hydrolab DS5X pH sensors were calibrated with a routine two-point calibration using
202 NIST buffers of pH_{NBS} 7.0 and 10.0. Before and after each deployment all instruments were placed
203 in a 50 liter tank with sea water to intercalibrate sensors. All pH loggers were offset to the same
204 newly calibrated high-precision SeaFET pH sensor, calibrated at the Satlantic facility
205 (www.satlantic.com) on the total scale using single-point calibration. Oxygen sensors were
206 calibrated to O_2 concentrations of the tank as determined from Winkler titrations.
207
208 To monitor three-dimensional pH variations on a m-scale within the kelp canopy, we deployed a
209 custom built multi-sensor array, consisting of an autonomous data logger (Datataker DT85) in a
210 water-tight housing (custom built by Albatros Marine Technologies S.I.) with 16 pre-amplified pH
211 electrodes (Omega, PHE-1304-NB). The pH sensors were attached to the submersible logger by 5
212 m long cables to allow for adjusting their position as needed (Fig. A1). The sensors were configured
213 in situ in a three dimensional array on the metal frame occupying a volume of approximately 1 m^3,
214 with 4 sensors at 0.1 m from the bottom, 4 sensors at 0.2 m, 4 sensors just underneath the canopy

and 4 above the canopy, which typically extended about 0.75 m above the seafloor. All pH sensors were calibrated with a three point calibration using NIST buffers of pH_{NBS} 4.0, 7.0 and 10.0 allowing at least 5 min between every reading for the sensors to stabilize. All pH loggers were offset to the same newly calibrated high-precision SeaFET pH sensor as mentioned above. On several occasions triplicate samples for determination of C_T and A_T were collected and analyzed as described above to allow calculation of carbonate chemistry and Ω_{arag}.

pH-variation in vegetated tidal pools dominated by *Ascophyllum nodosum* and adjacent intertidal habitats on the shore also dominated by *A. nodosum* and *Fucus* spp. were quantified over a diurnal cycle through sampling at low tide just after pool formation and prior to pool inundation during day and night. pH and Ω_{arag} were calculated from C_T and A_T samples collected and analyzed as described above and computed using the CO2SYS program (Pierrot et al., 2006) with in situ information on temperature and salinity. Salinity was analysed from water samples based on measurements of conductivity (Orion 3 STAR Conductivity benchtop) while oxygen concentration and water temperature were determined using a portable meter (Hack, HQ40d).

2.4. Micro-scale pH variation

pH-variations at a millimeter scale were measured in the laboratory on 6 different species of macrophytes (the intertidal brown macroalgae *Ascophyllum nodosum* and *Fucus vesiculosus*, the kelps *Saccharina longicruris* and *Agarum clathratum*, the green alga *Ulva lactuca*, and the seagrass *Zostera marina*) occurring in Kobbefjord and collected either there or, for logistic reasons, in another branch of the Godthåbsfjord system. From each species, a piece of approximately 5 x 2 cm was cut and mounted on a microscope slide in an aquarium with seawater before measurements. The set-up was mounted in an aquarium in a climate-controlled room with temperature kept at 2-

239 3ºC. By gently blowing the water surface above the mounted slide with air supplied by an
240 aquarium pump, we generated a stable, low, current velocity of approximately 0.28 ± 0.02 (SE) mm
241 s^{-1} in our observational area. We measured pH from a point close to the leaf surface up until out of
242 the diffusive boundary layer where the pH was stable. We used UNISENSE micro-pH sensors with
243 25 or 50 µm tips, connected to a Volt meter with 1 decimal precision for mV measurements
244 (Consort, R362). pH sensors were calibrated with a three point calibration using NIST buffers of
245 pH_{NBS} 4.0, 7.0 and 10.0 before each series of measurements. After each change in species or replica
246 a resting period of >15 min was observed to allow the diffusive boundary layer to be fully
247 developed before measurements. A USB microscope (Dinocapture) connected to a PC with on-
248 screen visualization software aided in visually establishing the lowest point of the measurements, as
249 close to the macrophyte surface as possible without breaking the tip of the electrode. A scaled
250 picture from this lowest point allowed for back calculating the actual distance to the leaf surface
251 afterwards. We allowed readings at this lowest point to stabilize for >5 min after which the mV
252 value was written down manually. The microsensor was then raised 20 µm with a precise 1D
253 micromanipulator, afterwards 30 µm, after which we continued with 50 µm increments and then
254 100 and 500 µm increments until a stable pH was obtained for 3 measurements or more and we
255 considered we were outside the diffusive boundary layer, between subsequent points the sensor was
256 allowed to stabilize for at least 5 min. We evaluated 3 replicas of each species at a irradiance of 200
257 µmol photons m^{-2} s^{-1}, and calculated the Δ pH across the diffusive boundary layer (defined from the
258 tissue surface to where pH was at 0.99 × water-column pH).
259
260 **3. Results**
261
262 Data are available in digital form (Krause-Jensen et al., 2015).
263
264 *3.1. Fjord-scale and seasonal pH variability*

Large seasonal and spatial variability was observed in pH-values along the longitudinal gradient centrally in the fjord (Fig. 2a). pH_T in surface water increased in April due to CO_2 consumption by the spring bloom as evidenced by a very high fluorescence (Fig. A2), to a maximum value of almost 8.50, most pronounced in the mouth of the fjord with values of around 8.25 in the inner part (Fig. 2). Accordingly, a horizontal gradient of around 0.25 pH units was observed along the main axis of the fjord. pH_T values in upper layers decreased during the summer to around 8.35 in July and with the maximum observed towards the inner part of the fjord. A further decrease in pH was observed in September, with more homogenous values in surface waters along the fjord gradient resulting in a horizontal range of only 0.05 pH units. Vertical gradients in pH from the surface to the deeper waters of the fjord ranged from only 0.1 units in April, when the fjord was vertically mixed, over 0.15 units in September to 0.25 pH units in July when maximum pH_T values of 8.35 occurred in a subsurface algal bloom in the inner parts of the fjord with waters supersaturated in oxygen (up to 120 % saturation, Fig. A2, A3) and minimum values of pH_T 8.1 were measured in the deeper sectors (Fig. 2a). Seasonally pH varied between 0.2 and 0.3 units in both surface and deep waters over the 5 months. Ω_{arag} values were closely coupled to pH and ranged from minimum values of 1.6, observed in the bottom waters of the inner part of the fjord, to maximum values of 2.5 in the subsurface waters in September (Krause-Jensen et al., 2015). Corresponding pCO_2 levels ranged from 162 to 325 µatm, in the range of values recently reported for the fjord (Sejr et al., 2014).

Oxygen saturation at the fjord-scale ranged greatly from 85% to 127% and was strongly related to pH for each of the three periods (Fig. 3a), pointing at strong biological control of pH variability within the fjord. The slope of the pH versus O_2 relationship was steepest for the April survey when the highest pH levels were observed. Examination of pH values in relation to fluorescence and temperature also showed that the warmest waters, of up to 10 ^{o}C, observed in July, supported

intermediate pH, while the highest pH was observed in the coldest waters, corresponding to the April survey when temperatures were uniformly low across the fjord (Fig. 3b). On a vertical scale, the cold bottom waters with low fluorescence generally supported the lowest pH values across seasons. Hence, overall, pH showed much tighter correlation with O_2 levels than with water temperature, and the correlation between pH and O_2 implied a similar close correlation between Ω_{arag} and O_2-levels.

3.2. Small-scale and diurnal pH- variability in kelp forests and benthic habitats colonized by microalgae/scattered filamentous algae

The 3 parallel deployments in kelp forest and habitats colonized by microalgae and scattered filamentous algae encompassed 6 complete diurnal cycles which exhibited peak pH_T-levels during the day of 8.11 (8.04-8.19) (avg. (s.d)) and of 8.08 (8.02-8.16), respectively, as opposed to minimum pH_T-levels during night of 8.02 (7.97-8.06) and 8.01 (7.94-8.09), respectively, with no significant difference between habitats (t-test, $p>0.05$). The diurnal range of minimum night pH to maximum day pH was slightly higher in the kelp forest (avg.±s.d. = 0.098±0.061) than above the microalgae/filamentous algae (0.073±0.052) (paired, one-tailed t-test, $p=0.041$).

There were large differences in the extent of diel fluctuations in pH among deployments dependent on incident irradiance and the shifting phase of tidal state and the solar cycle (Fig. 4). Diel pH fluctuations were small during dark, cloudy days and when high tide coincided with peak solar radiation, thereby reducing incident irradiance on the benthic habitat. In contrast, diel pH fluctuations were amplified in deployments during sunny days when low tide coincided with peak solar radiation (Fig. 4). Hence, the interaction between tide and the solar cycle controlled incident radiation and thereby induced fluctuations in photosynthetic activity and pH. This was particularly

apparent in kelp forests where peak daily pH increased as a function of maximum daily photosynthetic solar radiation reaching the habitat during the day whereas this relationship was not significant in the water column above the microalgae/filamentous algae (Fig. 5). Indeed, biologic control of pH was also reflected in strong relationships between pH and O_2 concentration within each deployment in the kelp forests (R^2=0.64-0.76) particularly during high irradiance, as opposed to weaker pH versus O_2 relationships for the microalgae/filamentous algae sites (R^2=0.05-0.15) which also showed much smaller variability in O_2 levels (98-114% saturation) than did the kelp forest (92-128% saturation) (Fig. 6). The diurnal range of O_2 concentrations in the kelp forest matched the range recorded at pelagic fjord-scale on a seasonal basis (85-127%, Fig. 3).

Tidal changes in water masses, reflected by changes in salinity and temperature, also contributed to variations in pH and O_2 levels. This was visible as incidences of sudden changes in pH paralleling fluctuations in salinity and also as differences in pH levels between deployments in water masses of different salinity (Fig. 4). However, salinity explained much less of the variation in pH than did O_2, except in one deployment in the microalgae/filamentous algae habitat when salinity explained 51% of the variation in pH as opposed to 15% explained by O_2 (R^2=0.04-0.33 in kelp forest; R^2=0.04-0.51 in microalgae/filamentous algae, data not shown). So, overall biological activity had a much stronger influence on pH than had exchange of water masses.

The observed diurnal pH variability also translated into important fluctuations in Ω_{arag}, involving 0.18±0.06 units (from maximum day levels of 1.77±0.21 to minimum night levels of 1.60±0.17) in the kelp forest and 0.14±0.07 Ω_{arag} units (from maximum day levels of 1.72±0.30 to minimum night levels of 1.58±0.26) at the microalgae/filamentous algae sites. Corresponding pCO_2-levels ranged

336 from 238 to 536 µatm at the kelp sites and from 258 to 515 µatm at the microalgal/filamentous
337 algal sites.
338
339 *3.3. Meter to millimeter-scale pH variability in kelp forests*
340 Examination of the variability in pH within 1 m^3 kelp forest, sampled from the bottom of the
341 canopy to the overlying water column, using the multi-electrode array, showed very large
342 concurrent pH variability involving about 0.2 to 0.3 pH unit differences at any given time and with
343 a total pH_T range of 7.76-8.36 across deployments (Fig. 7). In general, pH tended to be highest at
344 the top of the canopy and in the water just above the canopy, reflecting that the canopy top is the
345 most photosynthetically active layer, while pH was generally lower in the shaded bottom part of the
346 canopy (Fig. 7) where photosynthetic biomass and incident irradiance are lower and respiration
347 rates higher. The range of pH within 1 m^3 of kelp forest at any one point in time was comparable
348 among deployments, despite the different light conditions, although the absolute values of pH
349 differed among deployments with highest levels observed at peak incident irradiance (Fig. 7). This
350 small-scale variability in pH also translated into a variability in Ω_{arag} of about 0.20 units in 1 m^3 of
351 habitat at any time.
352
353 pH also varied significantly within the diffusive boundary layer of the six macrophyte species
354 examined in the light (Fig. 8a), with pH increasing by 0.07-0.85 units, depending on species, from
355 the top of the 0.3-2.2 mm thick diffusive boundary layer to the surface of the plants (Fig. 8b).
356
357 *3.4. pH variability in intertidal pools*
358 pH and oxygen concentration showed important diel variability in vegetated intertidal pools, with
359 oxygen super-saturation (up to 176%) during the day and under-saturation (down to 11%) at night,

compared to far more uniform concentrations in the surface waters on the adjacent vegetated shore (89-111% saturation, Fig. 9). Accordingly, pH_T changed greatly in intertidal pools, reaching maximum values of 9.0 during the day and minimum values of 7.4 during night periods, i.e. a diel range of ca. 1.6 pH units. Diel pH fluctuations in the surface waters of the adjacent shore were much smaller (8.0-8.5) but still high, reflecting the metabolic activity of the intertidal vegetation growing on the shore (Fig. 9). The difference in pH between vegetated intertidal pools and adjacent shores provided an additional example of variability in pH between adjacent habitats.

4. Discussion

Our results highlight the nested scales of variability of pH present in the Kobbefjord ecosystem involving (1) seasonal variability, largely driven by the phytoplankton spring bloom as a major event affecting pH; (2) diel variability acting through complex changes in submarine irradiance modulating rates of photosynthesis and respiration of benthic vegetation driven by the interaction of the solar and the tidal cycles; (3) large-scale variability along horizontal and vertical fjord gradients reflecting gradients in metabolic activity in combination with movement of water masses, (4) variability between subtidal habitats with and without kelp forests and between vegetated tidal pools and adjacent vegetated shores reflecting variable degrees of biological control, (5) small-scale three dimensional variability due to heterogeneity in metabolic processes and mixing in vegetated habitats, and (6) micro-scale variability across the diffusive boundary layer of macrophytes (Fig 10).

Overall, metabolic processes played a fundamental role in driving pH-variability across scales, as reflected in strong relationships between oxygen concentration and pH at the fjord-scale and at both diel and seasonal scales. Primary producers played a major role in the regulation of pH-variability, both in the pelagic zone where, particularly, the intense spring bloom characteristic of Arctic

385 ecosystems (Takahashi et al., 2003, Sejr et al., 2014) induced high pH in the subsurface layers while
386 respiratory process in the bottom waters reduced pH; and in the nearshore benthic environment
387 where the presence of subtidal kelp forests and intertidal macroalgae induced marked spatial and
388 diurnal variability in pH. The mosaics of pH reflected that the density of the primary producers, and
389 the spatio-temporal separation of photosynthesis and ecosystem respiration in combination with
390 mixing of water masses were key drivers of the variability in both planktonic and benthic
391 communities. Hence, the vertical gradient of declining pH from upper illuminated to lower shaded
392 habitats varied from the 10-100 m scale in the planktonic community where the density of primary
393 producers is relatively low to the cm-m scale in dense kelp forests. The same is true on a temporal
394 scale where the diurnal pH variation in the benthic vegetation matches the seasonal variability of
395 pH in the planktonic community.
396
397 The scale of seasonal pH-variability in the planktonic community (Fig. 10) compared well with
398 previous reports for the Arctic, showing the spring bloom as a prevalent driver of pCO_2 (Sejr et al.,
399 2011, Meire et al. 2015). Though a multitude of factors including water depth, light regime, season,
400 seawater retention time, density and plant species may all affect pH variability in vegetated habitats,
401 our results match evidence from other latitudes of strong pH variability in macroalgal forests and
402 seagrass meadows. Hence, marked diel pH variability has also been reported from a Californian
403 kelp forest (Frieder et al., 2012), a Mediterranean seagrass bed (Hendriks et al. 2014), and in
404 extreme case for a temperate shallow dense algal bed (diel range ca. 1 unit, Middelboe and Hansen,
405 2007) and kelp forest (diel range: ca. 0.6-0.8 pH units, Cornwall et al. 2013a). Our pH
406 measurements in benthic habitats neighboring the kelp forest also carried a biological signal, though
407 less distinct, likely reflecting the combined signal of the benthic primary producers at the site, of the
408 neighboring kelp forests and of the planktonic community in the water masses exchanged with tidal

409 currents. The marked biological control of pH in kelp forests suggests that diel pH may be even
410 more pronounced during sunny days with more intense photosynthesis than during the generally
411 overcast conditions of our survey. Thus, while the identified pH range and pH vs. O_2-relationships
412 for the planktonic community covered the full growth season, they solely represented a few
413 overcast September days in the benthic habitats and would likely involve markedly higher levels
414 had they covered the full growth season. For sub-Antarctic giant kelp forests, the diel amplitude in
415 pCO_2 and C_T (Delille et al., 2009) during spring and summer as well as the seasonal amplitude in
416 pH, C_T and pCO_2 (Delille et al., 2000) were reported to be markedly higher within kelp forest as
417 compared with unvegetated habitats, underlining the kelps' strong biological control of pH.
418
419 We further show, for the first time, significant 3-d variability in pH within 1 m^3 of kelp forest, with
420 pH ranging about 0.2-0.3 pH units at any one point in time and a total variability across
421 deployments of 7.76-8.36 pH_T, resembling the range recorded across the entire growth season in the
422 pelagic. Levels of pH were dependent on the position in the kelp canopy, with the highest pH
423 generally appearing at the top of the canopy and decreasing toward the seafloor, likely reflecting the
424 vertical structure of photosynthetic activity in the kelp bed. The fast rates of metabolic activity in
425 combination with reduced flow in such densely vegetated habitats make these 3-D patterns appear
426 in spite of the marked exchange of water masses resulting from the 1-4.5 m tidal range.
427
428 Changes in pH were particularly pronounced in small tidal pools, where photosynthesis of dense
429 seaweed stands of primarily *Ascophyllum nodosum* and *Fucus* spp. drove O_2 levels to large
430 supersaturation levels (176%) and forced pH to extremes of up to pH_T 9.0 at low tide during sunny
431 days, corresponding to Ω_{arag} of 4.14 and pCO_2 of 13 µatm compared to night-values of pH_T 7.4,
432 Ω_{arag} of 0.27 and pCO_2 of 1647 µatm driven by community respiration which almost depleted O_2 in

433 the pools (11% saturation). In surface waters of adjacent densely vegetated intertidal shores, we
434 observed a maximum pH_T of 8.5 with corresponding Ω_{arag} 2.23 and pCO_2 of 96 µatm during the day
435 and a minimum pH_T of 8.0, with corresponding Ω_{arag} of 0.54 and pCO_2 of 243 µatm during the
436 night. While intertidal brown macroalgae thrive in such habitats when regularly flushed as in the
437 current study, apparently only *Ulva (Enteromorpha) intestinalis* occurs in isolated, rarely flushed
438 rock pools where it can drive pH to levels >10 (Björk et al., 2004).
439
440 At the micro-scale, pH also showed considerable variability with a range of up to 0.85 pH units
441 across the diffusive boundary layer of the key species of the vegetated shallow ecosystems, with
442 high pH levels at the tissue surface declining towards the bulk water during daytime (Fig. 8). There
443 was substantial variability among species, with intertidal macroalgae (*Ascophyllum* and *Fucus*)
444 showing the largest pH range. The interspecific differences likely related to the species'
445 photosynthetic rates as well as to their morphology, which affect the thickness of the diffusive
446 boundary layer (Hurd and Pilditch, 2011). This microscale pH variability across the diffusive
447 boundary layer compared well previous observations for the calcifying alga *Hamelida discoidea*
448 (pH range of 0.7 across diffusive boundary layer, de Beer and Larkum, 2001) as well as for the
449 coralline algae *Sporolithon durum* (light-dark pH change at tissue surface 0.9; Hurd et al., 2011)
450 and *Arthrocardia corymbosa* (pH range across diffusive boundary layer e.g. 0.4, depending on
451 flow; Cornwall et al., 2013b). The pH range across the diffusive boundary layer of Ulva was
452 surprisingly low considering the ability of Ulva to elevate pH to high levels (Björk et al. 2004) but
453 probably the combination of low water temperature and limited nutrient supply limited the
454 photosynthetic rate. The diffusive boundary layer thickness as well as the pH range across it
455 depends markedly on flow conditions. Reduced flows as present in dense vegetation increase the
456 diffusive boundary layer thickness and consequently the pH range (Hurd et al., 2011, Cornwall et

al., 2013b). The current experiment was, hence, conducted at reduced flow, and, importantly, at the same flow for all species. Exchange of water masses with different salinity and temperature also added to the variability in pH as indicated for both pelagic (Fig. 3B) and benthic (Fig. 4) systems but showed much weaker correlation to pH than did O_2 concentrations reflecting the biological control.

The processes above resulted in nested scales of pH variability in the Kobbefjord ecosystem (Fig. 10), with variability ranging 0.2-0.85 units across spatial scales and 0.2-1.6 units over diurnal to seasonal scales. This variability provides a dynamic mosaic of niches for organisms. Niches of high pH may be particularly important for the more vulnerable larval and juveniles stages of calcifiers under conditions of low pH as projected for the future (Kroecker et al., 2013). The suitability for calcifiers is best represented by Ω_{arag}, where calcifiers should be favored by high Ω_{arag} values. The Kobbefjord ecosystems host a number of calcifying species, including bivalves such as blue mussel, scallops and snails, echinoderms, such as green sea urchins, and crustaceans such as *Pseudobalanus balanoides*, calcareous algae and foraminifers. Overall, the identified Ω_{arag} conditions were well above 1, particularly in illuminated habitats with intense photosynthesis and, hence, indicated favorable conditions for calcification. The phytoplankton spring bloom, depleting CO_2 and driving Ω_{arag} to values close to 3, would also provide adequate conditions for pelagic calcifiers, as it would provide the double benefit of adequate environments for aragonite deposition and food supply to support growth and the energetic demands of calcifiers. Canopies of kelp and intertidal seaweed environments may also provide adequate niches for calcifiers during summer, when Ω_{arag} values would be highest through the cumulative action of the processes upregulating pH and Ω_{arag} values discussed above. Indeed, most calcifiers spawn and recruit in early summer (Arendt et al. 2013)

480 when pCO_2 remains low, warmer water temperatures lead to higher Ω_{arag} and high solar radiation
481 and long photoperiod allow seaweeds to draw down CO_2 further (Delille et al., 2000).
482
483 The upregulating effect of primary producers on pH is counterbalanced by the opposite effect of
484 respiration and decomposition prevailing in shaded and deeper basins and periods as illustrated by
485 the large scale seasonal variability in the pelagic community (Fig. 2), and paralleled in kelp forests
486 outside the productive period (Delille et al., 2009) as well as during night time and in shaded layers
487 of the kelp forest (Fig. 7) and tidal pools (Fig. 9). These shaded habitats with diurnally low Ω_{arag}
488 could be challenging habitats for calcifyers. Interestingly, however, blue mussels grew in close
489 association with macroalgae even in intertidal pools, where they would experience maximum Ω_{arag}
490 values of up to 4.28 when low tide occurred at noon as opposed to levels as low as 0.28 during
491 night (Fig. 9). Blue mussels have indeed been observed to abound in intertidal macroalgal habitats
492 (Blicher et al. 2013) and along with other calcifiers to be trophically linked with habitat-forming
493 algae such as *Ascophyllum* (Riera et al., 2009), and have also been reported to tolerate high pCO_2
494 concentrations when food is abundant (Thomsen et al., 2013). Probably the recurring periods of
495 high Ω_{arag} in combination with adequate food supply can compensate for the potential problems of
496 low Ω_{arag} during night. Laboratory experiments have demonstrated that semidiurnal fluctuations of
497 0.3 pH units may compensate for negative effects of constantly low pH on the development of
498 mussel larvae (Frieder et al. 2014). Calcareous epiphytic organisms, such as encrusted algae and
499 bryozoans would also experience high variability in Ω_{arag} at the surface of the plant tissue, where
500 periodically high Ω_{arag} values favors calcification, as elegantly demonstrated by de Beer and
501 Larkum (2001).
502

The existence of a mosaic of environments in the Kobbefjord underlines the importance of metabolic processes along with habitat configuration and interactions among community constituents in affecting pH in coastal ecosystems as opposed to the simpler situation in the open ocean (Duarte et al., 2013, Hendriks et al., 2014). This pronounced influence of metabolic processes occurs in spite of Kobbefjord being a macrotidal area with marked exchange of water masses with the coastal region and is probably also the case in many other shallow coastal areas in the Arctic, as has also been highlighted for areas in the temperate zone (Duarte et al., 2013). While the current study explored pH in benthic habitats under overcast situations in the early autumn of the sub-Arctic, kelp forests are likely to induce much more pronounced increases in pH and Ω_{arag} in midsummer when irradiances are higher and the photoperiod longer, and further north, during high-Arctic midsummer, when the sun does not set for months. Under scenarios of ocean acidification such vegetated habitats may gain increased importance as local refuges for calcifyers. The projected poleward expansion of macrophytes into the Arctic with warming and reduced sea ice cover (Müller et al. 2009, Jueterbock et al. 2013) has been hypothesized to provide such niches of elevated pH and Ω_{arag} during summer (Krause-Jensen et al. 2014). Similarly, increased pelagic primary production as forecasted for parts of the Arctic Ocean (Arrigo et al., 2008; Slagstad et al., 2011, Popova et al., 2012) may also create local niches of high pH.

5. Acknowledgements

The study was funded by the Danish Environmental Protection Agency within the Danish Cooperation for Environment in the Arctic (DANCEA). L. Meire was funded by the Research foundation Flanders (FWO aspirant grant) and by Defrost under the Nordic Centers of Excellence (NCoE) program. O. Geertz-Hansen, Greenland Climate Research Centre, /Greenland Institute of

Natural Resources, Nuuk, is thanked for help with field work. The study is also a contribution to the Greenland Ecosystem Monitoring program (www.G-E-M.dk) and the Arctic Science Partnership (ASP) asp-net.org.

6. Author contributions

Planning, field work, data processing and writing were carried out jointly, led by D. Krause-Jensen and C. M. Duarte, with L. Meire and M. K. Sejr responsible for fjord-scale surveys, I. E. Hendriks, M. K. Sejr, M. E. Blicher, C. M. Duarte and D. Krause-Jensen responsible for the various small scale measurements, I. E. Hendriks and N. Marba for micro-scale measurements, N. Marba and D. Krause-Jensen for intertidal measurements and M. E. Blicher for Greenland field facilities. Main idea: C. M. Duarte.

7. References

AMAP: AMAP Assessment 2013: Arctic Ocean Acidification, Arctic Monitoring and Assessment Programme (AMAP), Oslo, Norway, viii + 99 pp., ISBN – 978-82-7971-082-0, 2013.

Arendt, K.E., Juul-Pedersen, T., Mortensen, J., Blicher, M.E. and Rysgaard, S: A 5-year study of seasonal patterns in mesozooplankton community structure in a sub-Arctic fjord reveals dominance of *Microsetella norvegica* (Crustacea, Copepoda). Journal of Plankton Research 35(1):105-120, doi: 10.1093/plankt/fbs087, 2013.

Arrigo, K.R., van Dijken, G., and Pabi, S.: Impact of a shrinking Arctic ice cover on marine primary production, Geophys. Res. Lett., 35, 1–6, 2008.

Attard, K.M., Glud, R.N., McGinnis, D.F. and Rysgaard S.: Seasonal rates of benthic primary production in a Greenland fjord measured by aquatic eddy correlationLimnol. Oceanogr., 59(5), 1555–1569, 2014.

Blicher, M. E., Rasmussen, L. M., Sejr, M. K., Merkel, F. R. and Rysgaard, S.: Abundance and energy requirements of eiders (Somateria spp.) suggest high predation pressure on macrobenthic fauna in a key wintering habitat in SW Greenland, Polar Biol., 34, 1105–1116, doi:10.1007/s00300-011-0968-3, 2011.

Blicher, M. E., Rysgaard, S. and Sejr, M. K.: Growth and production of sea urchin Strongylocentrotus droebachiensis in a high-Arctic fjord, and growth along a climatic gradient (64 to 77 degrees N). Mar. Ecol. – Prog. Ser., 341, 89-102, 2007.

Blicher, M. E. and Sejr, M. K.: Abundance, oxygen consumption and carbon demand of brittle stars in Young Sound and the NE Greenland shelf, Mar. Ecol. Prog. Ser., 422, 139–144, doi:10.3354/meps08915, 2011.

Blicher, M.E., Sejr, M.K., and Høgslund, S.: Population structure of *Mytilus edulis* in the intertidal zone in a sub-Arctic fjord, SW Greenland, Mar. Ecol. Prog. Ser., 487, 89-100, 2013.

Blicher, M. E., Sejr, M. K. and Rysgaard, S.: High carbon demand of dominant macrozoobenthic species indicates their central role in ecosystem carbon flow in a sub-Arctic fjord, Mar. Ecol. Ser., 383, 127–140, doi:10.3354/meps07978, 2009.

Björk, M., Axelsson, L., and Beer, S.: Why is *Ulva intestinalis* the only macroalga inhabiting isolated rock pools along the Swedish Atlantic coast? Mar. Ecol. Prog. Ser., 284, 109–116, 2004.

Connell, S., Russell, B.D.: The direct effects of increasing CO_2 and temperature on non-calcifying organisms: increasing the potential for phase shifts in kelp forests. Proc. R. Soc. B 277, 1409-1415, 2010.

Cornwall, C.E., Hepburn, C.D., McGraw, C.M., Currie, K.I., Pilditch, C.A., Hunter, K.A., Boyd, P.W., and Hurd, C.L.: Diurnal fluctuations in seawater pH influence the response of a calcifying macroalga to ocean acidification. Proc. R. Soc. B 80: doi:10.1098/rspb.2013.2201, 2013a.

Cornwall, C.E., Hepburn, C.D., Pilditch, C.A., and Hurd, C.L.: Concentration boundary layers around complex assemblages of macroalgae: Implications for the effects of ocean acidification on understorey coralline algae. Limnol. Oceanogr. 58, 121-130, 2013b.

De Beer, D. and Larkum, A.W.D.: Photosynthesis and calcification in the calcifying algae *Halimeda discoidea* studied with microsensors, Plant Cell Environ., 24, 1209–1217, 2001.

Delille, B., Delille, D., Fiala, M., Prevost, C., and Frankignoulle, M.: Seasonal changes of pCO_2 over a subantarctic Macrocystis kelp bed, Polar Biol., 23, 706–716, 2000.

Delille, B., Borges, A.V., and Delille, D.: Influence of giant kelp beds (*Macrocystis pyrifera*) on diel cycles of pCO_2 and DIC in the Sub-Antarctic coastal area, Estuar. Coast Shelf Sci., 81, 114–122., doi:10.1016/j.ecss.2008.10.004, 2009.

Dickson, A. G., Sabine, C. L., and Christian, J. R.: Guide to best practices for ocean CO_2 measurements, PICES Special Publication, 191 pp., 2007.

Dickson, A.G., and Millero, F.J.: A comparison of the equilibrium constants for the dissociation of carbonic acid in seawater media, Deep-Sea Res., 34, 1733-1743, 1987.

Duarte, C., Hendriks, I., Moore, T., Olsen, Y., Steckbauer, A., Ramajo, L., Carstensen, J., Trotter, J., and McCulloch, M.: Is Ocean Acidification an Open-Ocean Syndrome? Understanding Anthropogenic Impacts on Seawater pH, Estuar. Coast., 36, 221–236, 2013.

Fabry, V. J., McClintock, J. B., Mathis, J. T., and Grebmeier, J. M.: Ocean Acidification at High Latitudes: The Bellweather. Oceanogr. 22, 160-171, 2009.

Frieder, C. A., Nam, S. H., Martz, T. R., and Levin, L. A.: High temporal and spatial variability of dissolved oxygen and pH in a nearshore California kelp forest, Biogeosciences, 9, 3917–3930, doi:10.5194/bg-9-3917-2012, 2012.

Frieder, Christina A., Gonzales, J.P., Bockmon, E.E., Navarro, M.O., Levini, L.A.: Can variable pH and low oxygen moderate ocean acidification outcomes for mussel larvae? Glob. Change Biol., 20, 754-764, doi: 10.1111/gcb.12485, 2014.

Glud, R.N., Berg, P., Hume, A., Batty, P., Blicher, M.E., Lennert, K., and Rysgaard, S.: Benthic O_2 exchange across hard-bottom substrates quantified by eddy correlation in a sub-Arctic fjord, Mar. Ecol. –Prog. Ser., 417, 1–12, doi: 10.3354/meps08795, 2010.

Helm, V., Humbert, A. and Miller, H.: Elevation and elevation change of Greenland and Antarctica derived from CryoSat-2, Cryosph., 8(4), 1539–1559, doi:10.5194/tc-8-1539-2014, 2014.

Hendriks, I. E., Olsen, Y. S., Ramajo, L., Basso, L., Steckbauer, A., Moore, T. S., Howard, J., and Duarte, C. M.: Photosynthetic activity buffers ocean acidification in seagrass meadows, Biogeosciences, 11, 333-346, doi:10.5194/bg-11-333-2014, 2014.

Hofmann, G.E., Smith, J.E., Johnson, K.S., Send, U., Levin, L.A., Micheli, F., Paytan, A., Price, N. N., Peterson, B., Takeshita, Y., Matson, P. G., Crook, E. D., Kroeker, K. J.., Gambi, M. C., Rivest, E. B., Frieder, C. A., Yu, P. C., and Martz, T. R.: High-Frequency Dynamics of Ocean pH: A Multi-Ecosystem Comparison. PLoS ONE 6(12): e28983, doi:10.1371/journal.pone.0028983, 2011.

Hurd, C.L., Cornwall, C.E., Currie, K., Hepburn, C.D., McGraw, C.M., Hunter, K.A., and Boyd P.W.: Metabolically-induced pH fluctuations by some coastal calcifiers exceed projected 22nd century ocean acidification: a mechanism for differential susceptibility? Glob. Change Biol., 17: 3254–3262, doi:10.1111/j.1365-2486.2011.02473.x, 2011.

Hurd, C.L. and Pilditch ,C.A.: Flow-induced morphological variations affect diffusion boundary-layer thickness of *Macrocystis pyrifera* (Heterokontophyta, Laminariales). J. Phycol. 47, 341-351, 2011.

Høgslund, S., Sejr, M.S., Wiktor, J. Jr., Blicher, M.E., and Wegeberg, S.: Intertidal community composition along rocky shores in Southwest Greenland: a quantitative approach, Polar Biol. 37, 1549–1561, doi 10.1007/s00300-014-1541-7, 2014.

Jueterbock, A.,Tyberghein, L.,Verbruggen, H.,Coyer, J.A., Olsen, J.L., and Hoarau,G.: Climate change impact on seaweed meadow distribution in the North Atlantic rocky intertidal. Ecol. Evol. 3, 1356–1373. doi: 10.1002/ece3.541, 2013.

Krause-Jensen, D. and Duarte, C.M. Expansion of vegetated coastal ecosystems in the future Arctic. Front. Mar. Sci., 1:77, doi:10.3389/fmars.2014.00077, 2014.

Krause-Jensen, D., Marbà, N., Olesen, B., Sejr, M.K., Christensen, P.B., Rodrigues, J., Renaud, P.E., Balsby, T.J.S., and Rysgaard, S.: Seasonal sea ice cover as principal driver of spatial and temporal variation in depth extension and annual production of kelp in Greenland, Glob. Change Biol., 18, 2981–2994, 2012.

Krause-Jensen, D., Duarte, C. M., Hendriks, I. E., Meire, L., Blicher, M. E., Marbà, N., and Sejr, M. K.: Nested scales of pH variability in sub-Arctic Kobbefjord, SW Greenland", DIGI-TAL.CSIC, available at: http://hdl.handle.net/10261/112946, 2015.

Kroeker K.J., Kordas, R.L., Crim, R., Hendriks, I.E., Ramajos, L., Singh, G.S., Duarte, C.M., and Gattuso, J.-P.: Impacts of ocean acidification on marine organisms: quantifying sensitivities and interaction with warming, Glob. Change Biol., 19, 1884–1896, doi: 10.1111/gcb.12179, 2013.

Mehrbach, C., Culberson, C. H., Hawley, J. E., and Pytkowicz, R. M.: Measurement of the apparent dissociation constants of carbonic acid in seawater at atmospheric pressure, Limnol. Oceanogr., 18, 897–907, 1973.

Meire, L., Søgaard, D. H., Mortensen, J., Meysman, F. J. R., Soetaert, K., Arendt K. E., Juul-Pedersen T., and Rysgaard, S.: Glacial meltwater and primary production as drivers for strong CO_2 uptake in fjord and coastal waters adjacent to the Greenland Ice Sheet. Biogeosciences 10.5194/bg-12-2347-2015.

Mercado J.M., and Gordillo F.J.: Inorganic carbon acquisition in algal communities: are the laboratory data relevant to the natural ecosystems? Photosynth. Res. 109, 257–267, doi: 10.1007/s11120-011-9646-0, 2011.

Middelboe, A. L., and Hansen, P. J.: Direct effects of pH and inorganic carbon on macroalgal photosynthesis and growth, Mar. Biol. Res., 3, 134–144, 2007.

Müller, R., Laepple, T., Bartsch,I., and Wiencke, C. Impact of oceanic warming on the distribution of seaweeds in polar and cold-temperate waters. Bot.Mar., 52, 617–638, doi:10.1515/BOT.2009.080, 2009.

Olesen, B., Krause-Jensen, D., Marbà, N., and Christensen, P.B.: Eelgrass (Zostera marina L.) meadows in subarctic Greenland: Dense meadows with slow biomass turnover. Mar. Ecol. Prog. Ser., 518, 107–121, doi: 10.3354/meps11087, 2015.

Olischläger M., Bartsch, I., Gutow, L., and Wiencke, C.: Effects of ocean acidification on different life-cycle stages of the kelp *Laminaria hyperborea* (Phaeophyceae). Bot. Mar. 55, 511–525, DOI: 10.1515/bot-2012-0163, 2012.

Pierrot, D. E. L., and Wallace, D. W. R.: MS Excel Program Developed for CO_2 System Calculations. ORNL/CDIAC-105a. Carbon Dioxide Information Analysis Center, Oak Ridge National Laboratory, U.S. Department of Energy, Oak Ridge, Tennessee. doi: 10.3334/CDIAC/otg.CO2SYS_XLS_CDIAC105a, 2006.

Popova, E. E., A. Yool, A. C. Coward, F. Dupont, C. Deal, S. Elliott, E. Hunke, M. Jin, M. Steele, and J. Zhang: What controls primary production in the Arctic Ocean? Results from an intercomparison of five general circulation models with biogeochemistry, J. Geophys. Res., 117, C00D12, doi:10.1029/2011JC007112, 2012.

Riera, P., Escaravage, C., and Leroux, C.: Trophic ecology of the rocky shore community associated with the Ascophyllum nodosum zone (Roscoff, France): a δ13C vs δ15N investigation. Estuar. Coast Shelf Sci., 81, 143-148, 2009.

Richter, A., Rysgaard, S., Dietrich, R., Mortensen, J., and Petersen, D.: Coastal tides in West Greenland derived from tide gauge records. Ocean Dyn. 61: 39–49, doi:10.1007/s10236-010-0341-z, 2011.

Sejr, M. K., Sand, M. K., Jensen, K. T., Petersen, J. K., Christensen, P. B. and Rysgaard, S.: Growth and production of Hiatella arctica (Bivalvia) in a high-Arctic fjord (Young Sound, Norhteast Greenland), Mar Ecol Prog Ser, 244, 163–169, 2002.

Sejr, M.K., Krause-Jensen, D., Rysgaard, S., Sørensen, L.L., Christensen, P.B., and Glud, R.N.: Air-sea flux of CO_2 in arctic coastal waters influenced by glacial melt water and sea ice, Tellus B, 63(5), 815-822, 10.1111/j.1600-0889.2011.00540.x, 2011.

Sejr, M.K., Krause-Jensen, D., Dalsgaard, T., Ruiz-Halpern, S., Duarte, C.M., Middelboe, M., Glud, R.N., Bendtsen, J., and Rysgaard, S.: Seasonal dynamics of autotrophic and heterotrophic plankton metabolism and pCO_2 in a subarctic Greenland fjord, Limnol. Oceanogr., 59(5), 1764–1778, 2014.

Slagstad,D., Ellingsen, I.H., and Wassmann, P: Evaluating primary and secondary production in an Arctic Ocean void of summer sea ice: an experimental simulation approach. Prog. Oceanogr. 90, 117–131.doi: 10.1016/j.pocean.2011.02.009, 2011.

Takahashi, T., Olafsson, J., Goddard, J. G., Chipman, D. W., and Sutherland, S. C.: Seasonal variation of CO_2 and nutrients in the high-latitude surface oceans: A comparative study. Global Biogeochem. Cy., 7, 843-878, 1993.

Thomsen, J., Casties, I., Pansch, C., Körtzinger, A., and Melzner, F.: Food availability outweighs ocean acidification effects in juvenile *Mytilus edulis*: laboratory and field experiments. Glob. Change Biol., 19, 1017-1027, 2013.

Uppström L.R.: The boron/chlorinity ratio of deep-sea water from the Pacific Ocean, Deep-Sea Res., 21, 161-162, 1974.

744 **Figure legends**

745 Fig. 1. A: Location of Kobbefjord, Nuuk. B: Location of sampling sites in Kobbefjord: Fjord scale
746 sites (CTD, C_T, A_T: filled circles; CTD: open circles), vegetated subtidal sites (open circles # 1-3),
747 and intertidal sites (open circles (#4). C: Photopanel of benthic habitats: A typical kelp forest
748 habitat (dominated by *Saccharina longicruris*) and habitat colonized by microalgae/scattered
749 filamentous algae (example from site #1, representative of sites #1-3 in map) and a vegetated
750 intertidal pool and the adjacent vegetated shore dominated by *Ascophyllum nodosum* and *Fucus*
751 spp. (site #4 in map).

752

753 Fig. 2. Fjord-scale pH-variability in Kobbefjord on 19 April, 18 July and 3 September 2013.

754

755 Fig. 3. Fjord-scale relationships in Kobbefjord between pH and oxygen (A), and between
756 temperature and fluorescence with associated pH-levels shown with symbol color (B), on three
757 sampling occasions: 19 April, 18 July and 3 September 2013.

758

759 Fig. 4. Diurnal variability in pH, O_2, water depth (all measured by Hydrolab) and irradiance
760 (measured by Odyssey loggers) at ca. 50 cm above the seafloor in kelp forests (Panels A-C) and
761 habitats colonized by microalgae/filamentous algae (panels E-F) during three parallel deployment in
762 Kobbefjord, Nuuk, 27-30 August, 30 August-2 September, 2-5 September 2013. The deployments
763 represent the benthic sites (#1-3, respectively) shown on the map (Fig. 1).

764

765 Fig. 5. Maximum daily pH in a kelp forest (green dots) and above microalgae/filamentous algae
766 (blue dots) as a function of maximum daily incident light over 6 full days as measured during three
767 parallel deployment in Kobbefjord, Nuuk, 27-30 August, 30 August-2, September, 2-5 September

2013. Linear fit and coefficient of determination shown for the significant relationship for the kelp forest.

Fig. 6. pH vs. O_2 concentration for three parallel deployments (#1-3 shown by increasing color intensity) in subtidal habitats colonized by kelp forests (top panel) or microalgae/scattered filamentous algae (bottom panels) in Kobbefjord, Nuuk, August-September 2013. Each deployment represents 10 min loggings by multiloggers (Hydrolab) over ca. 2 diurnal cycles. Linear fits and coefficients of determination are shown.

Fig. 7. pH-variability within 1 m^3 of kelp forest in Kobbefjord, Nuuk, during three deployments in late August-September 2013. 16 pH-sensors were configured in-situ in a 3-d array with 4 sensors at 0.1 m from the bottom, 4 sensors at 0.2 m, 4 sensors just underneath the canopy and 4 in the water column above the canopy, which typically extended about 0.75 m above the seafloor.

Fig. 8. Microscale pH-variability across diffusive boundary layers of blades of 6 different macrophyte species illuminated by 200 µmol photons m^{-2} s^{-1}: The kelps *Saccharina longicruris* and *Agarum clathratum*, the intertidal brown macroalgae: *Fucus vesiculosus* and *Ascophyllum nodosum*, the green macroalga *Ulva lactuca* and the seagrass *Zostera marina*. A: pH levels (mean of 2-3 replicate measurements) across blade diffusive boundary layers fitted by an exponential model ($y = y0 + a * exp^{-b*x}$, R^2>0.90 for all individual fits). B: pH range across the diffusive boundary layer of the various species.

Fig. 9. O_2-concentration and pH in vegetated tidal pools and in surface waters of neighboring vegetated intertidal shores measured at low tide during day and night just after pool formation and before pool inundation.

Fig. 10. Conceptual summary of nested scales of temporal and spatial variability in pH in Kobbefjord, Nuuk. The figure shows the maximum pH range at the various scales examined. From lower left to upper right: 1) micro-scale variability across macrophyte diffusive boundary layers, 2) small scale variability within kelp forests, 3) diurnal variability in vegetated subtidal habitats and intertidal pools/adjacent shores and variability between habitats at the 100 m scale, 4) seasonal and fjord-scale horizontal variability.

Appendix figures/Supplementary figures

Fig. A1. Photo of deployment frame with loggers shown on the deck of the boat (upper panel) and in situ in the *Saccharina longicruris*-dominated kelp forest (site #1, central panel). Markings in upper panel show the array of 16 pH sensors connected to a common pH logger, the hydrolab measuring salinity, temperature and oxygen and a PAR logger (odyssey).

Fig. A2. Fjord-scale variability in fluorescence in Kobbefjord, Nuuk, 19 April, 18 July and 3 September 2013.

Fig. A3. Fjord-scale variability in O_2-concentration in Kobbefjord, Nuuk, 19 April, 18 July and 3 September 2013.

Fig. 1

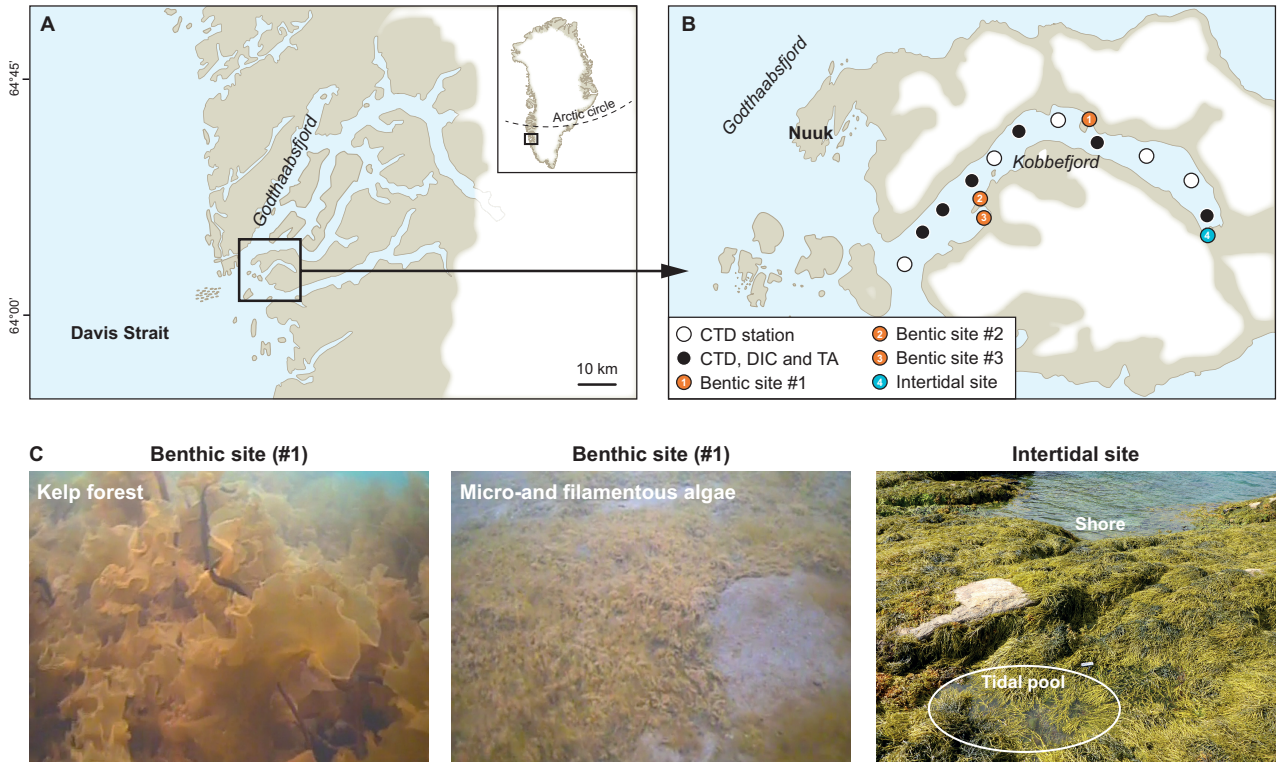
A
64°45'
64°00'
Godthaabsfjord
Davis Strait
Arctic circle
10 km
B
Godthaabsfjord
Nuuk
Kobbefjord
CTD station
CTD, DIC and TA
Bentic site #1
Bentic site #2
Bentic site #3
Intertidal site
C
Benthic site (#1)
Kelp forest
Benthic site (#1)
Micro-and filamentous algae
Intertidal site
Shore
Tidal pool

Fig. 2

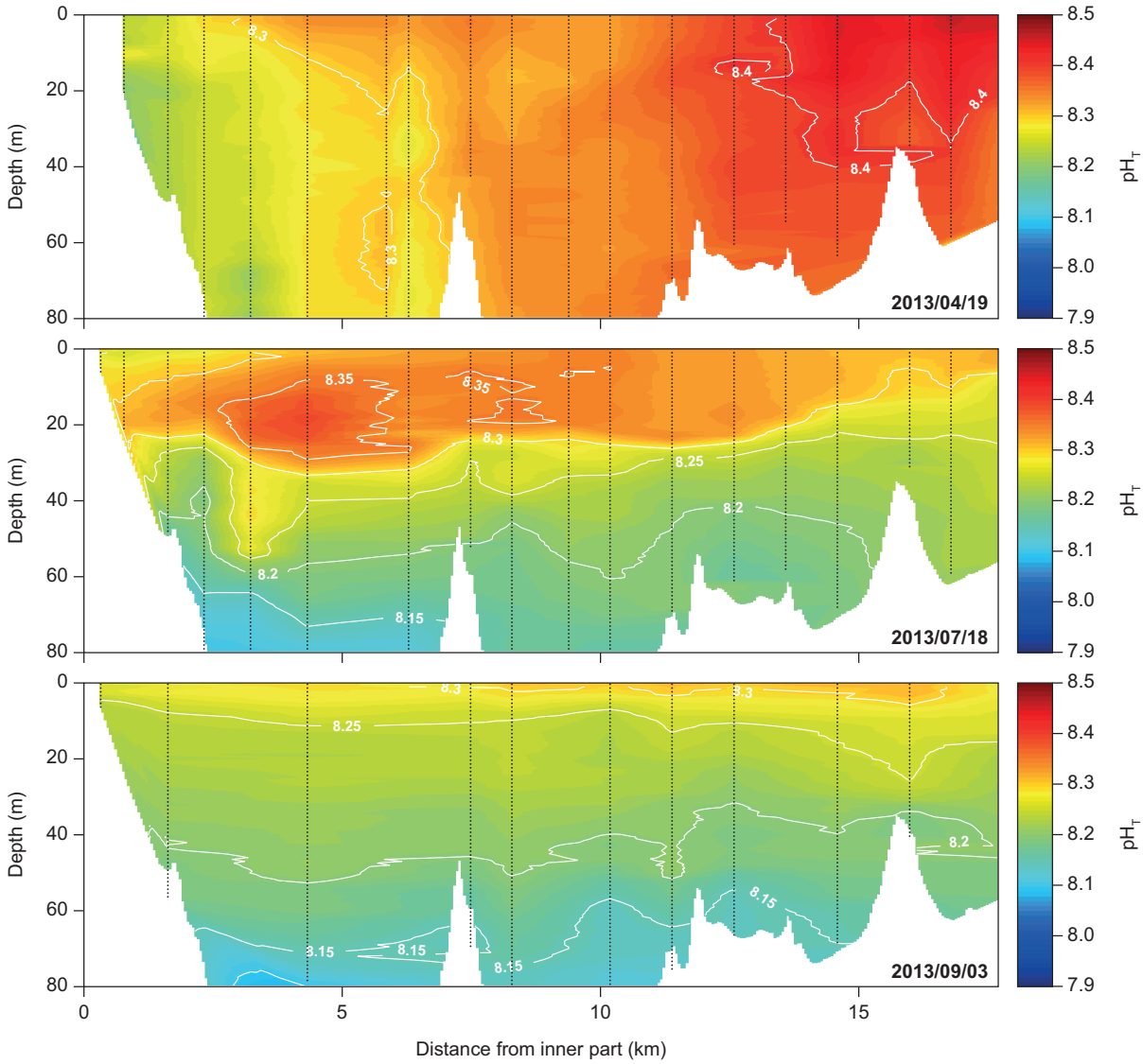
Depth (m)
0
20
40
60
80
8.3
8.4
8.4
8.4
8.3
2013/04/19
8.35
8.35
8.3
8.25
8.2
8.2
8.15
2013/07/18
8.3
8.3
8.25
8.2
8.15
8.15
8.15
8.15
2013/09/03
0
5
10
15
Distance from inner part (km)
8.5
8.4
8.3
8.2
8.1
8.0
7.9
pH$_T$

Fig. 3

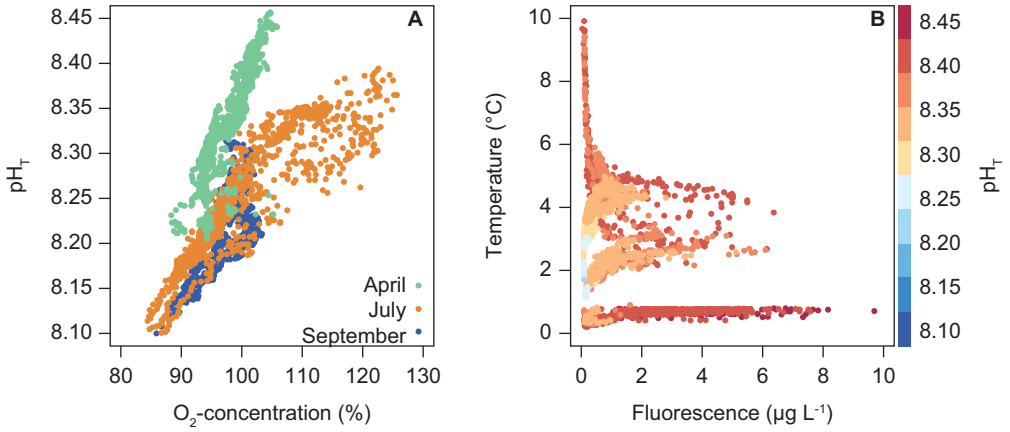
A
B
pH$_T$
8.45
8.40
8.35
8.30
8.25
8.20
8.15
8.10
80
90
100
110
120
130
O$_2$-concentration (%)
April
July
September
Temperature (°C)
10
8
6
4
2
0
Fluorescence (µg L^{-1})

823 Fig. 4

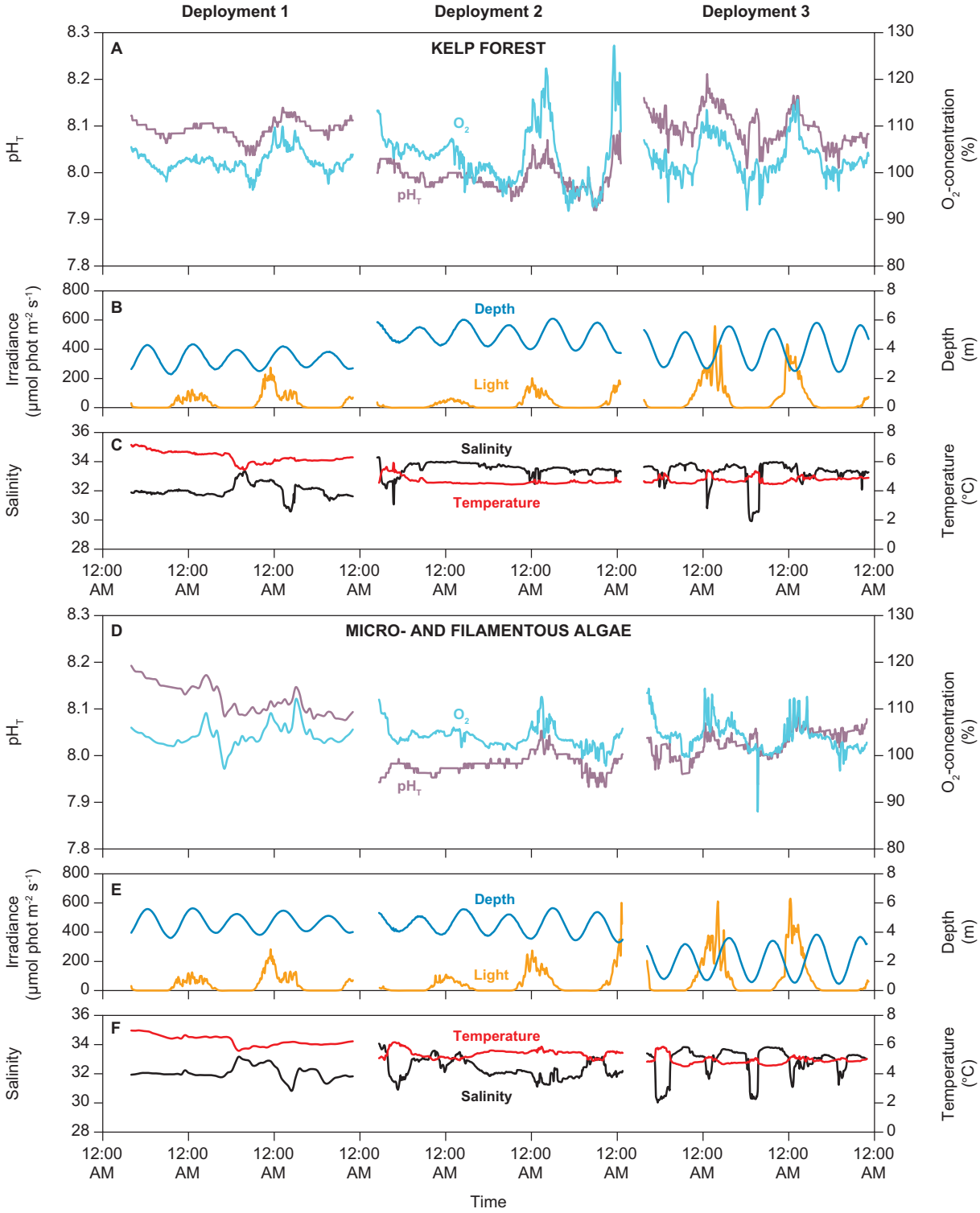

824

825

826 Fig. 5

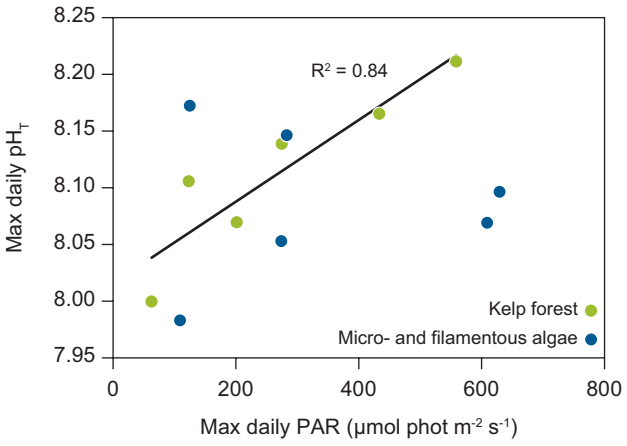

827

828

829 Fig. 6

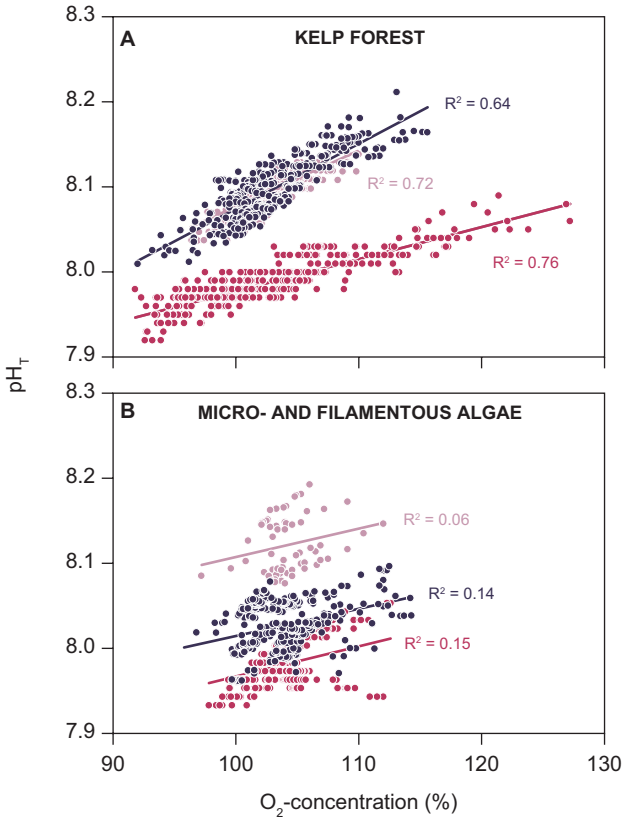

830

831

Fig. 7

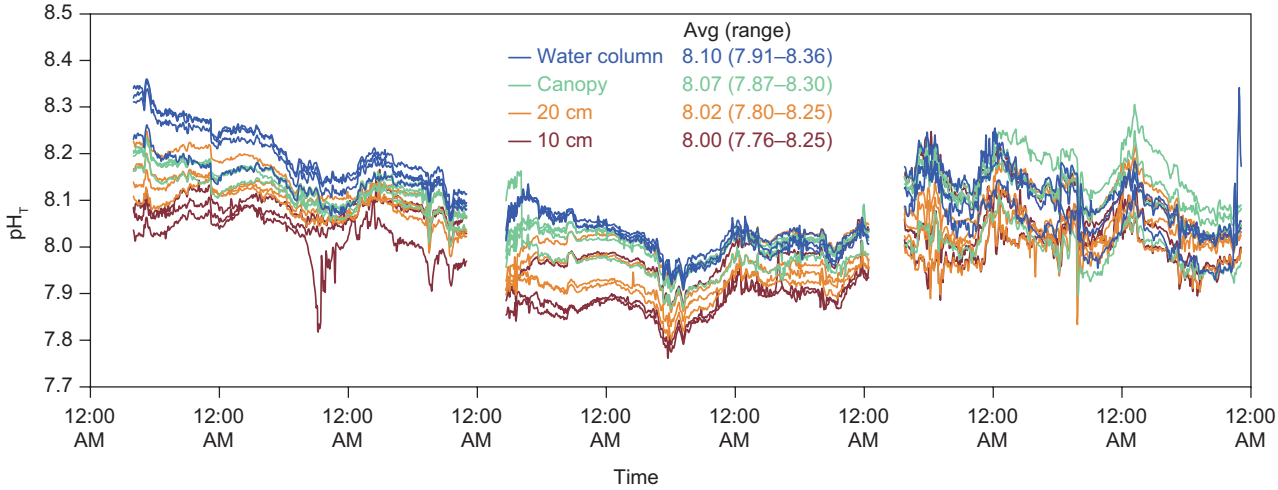
Avg (range)
Water column 8.10 (7.91–8.36)
Canopy 8.07 (7.87–8.30)
20 cm 8.02 (7.80–8.25)
10 cm 8.00 (7.76–8.25)
pH$_T$
8.5
8.4
8.3
8.2
8.1
8.0
7.9
7.8
7.7
12:00 AM
Time

835 Fig. 8

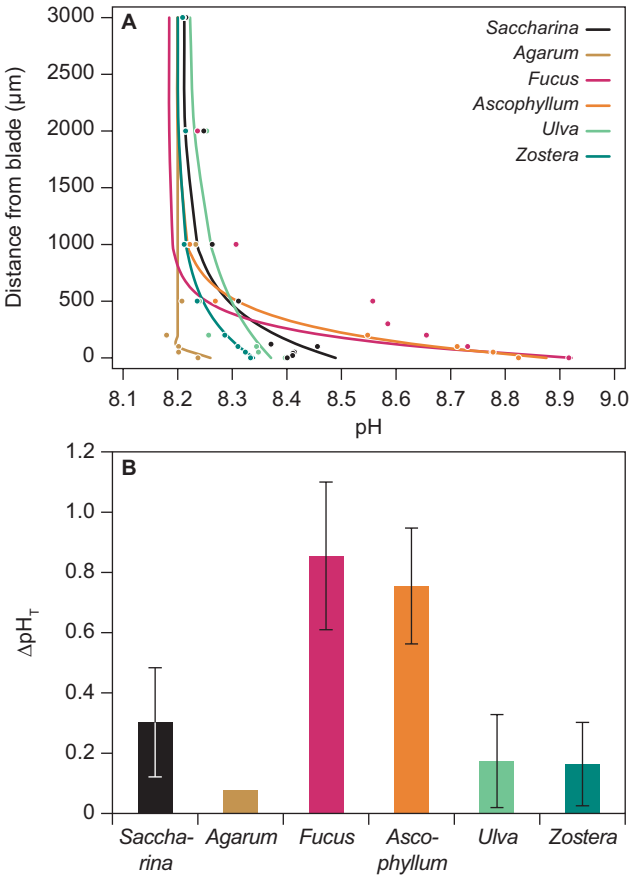

836

837

838 Fig. 9

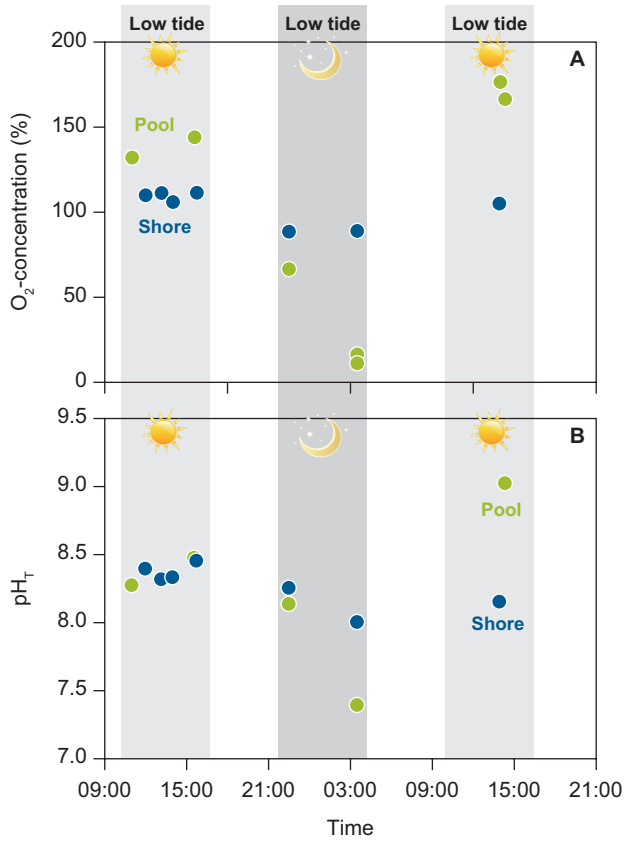

839

840

Fig. 10

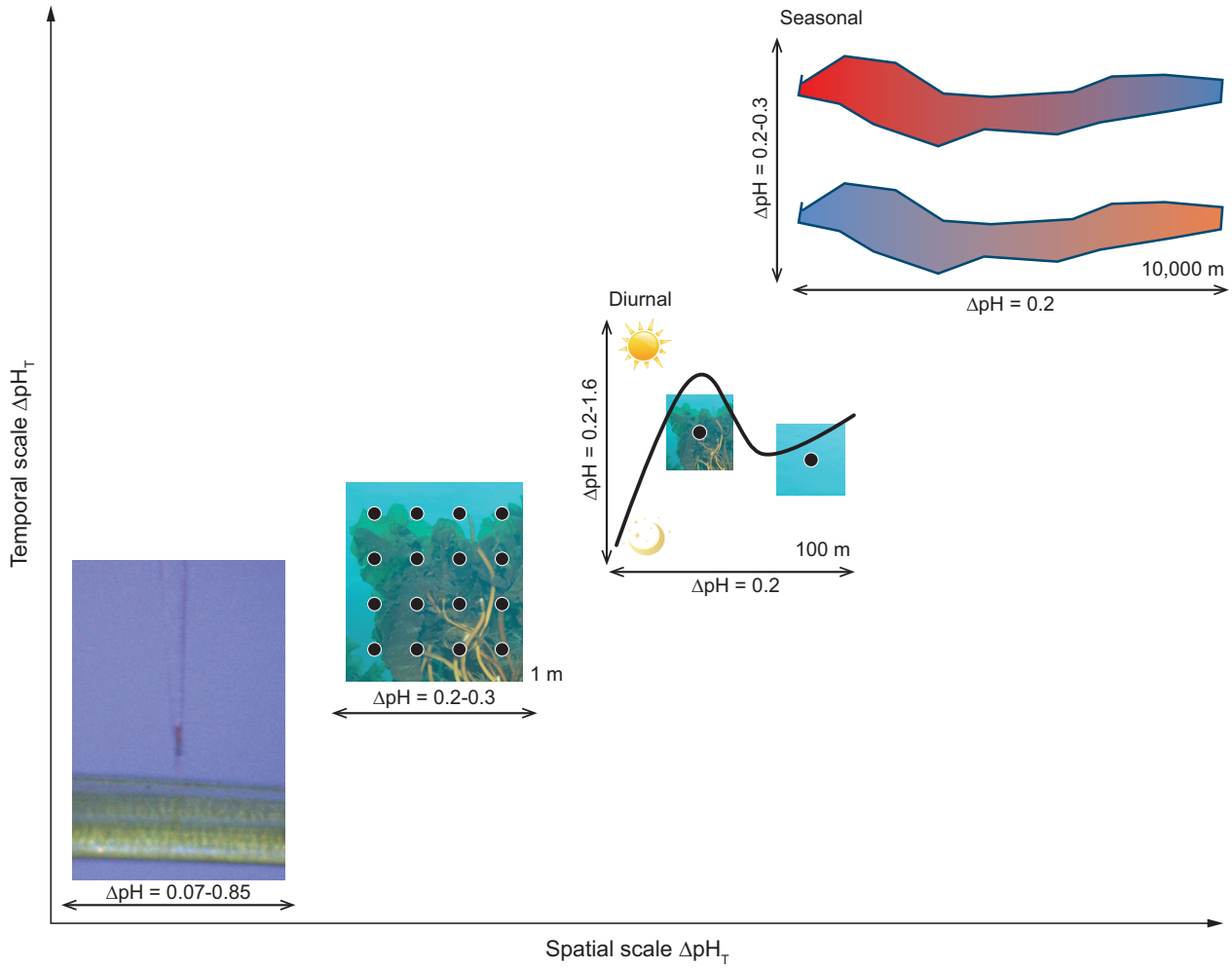
Seasonal
ΔpH = 0.2-0.3
10,000 m
ΔpH = 0.2
Diurnal
ΔpH = 0.2-1.6
100 m
ΔpH = 0.2
1 m
ΔpH = 0.2-0.3
ΔpH = 0.07-0.85
Temporal scale ΔpH$_T$
Spatial scale ΔpH$_T$

Appendix-figures/Supplementary figures

Fig. A1

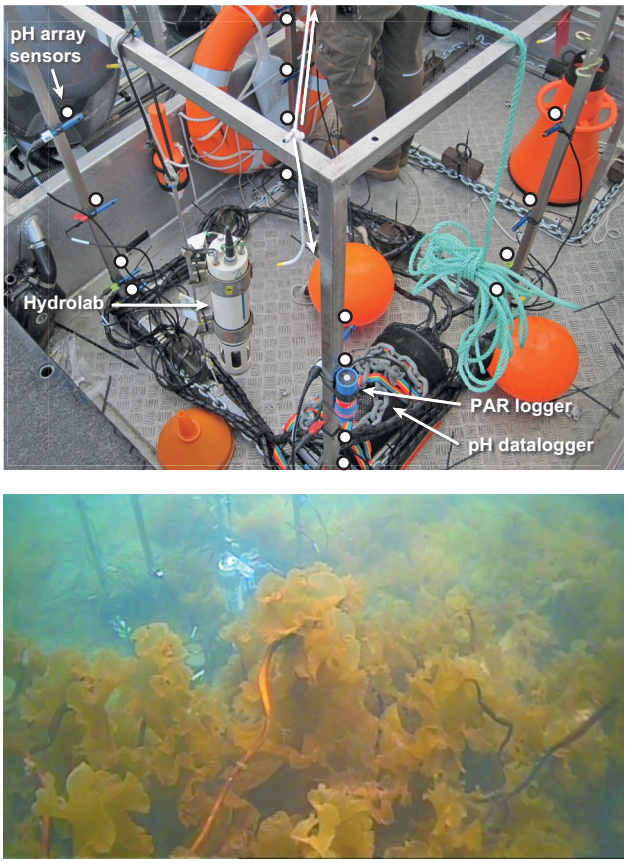

Fig. A2

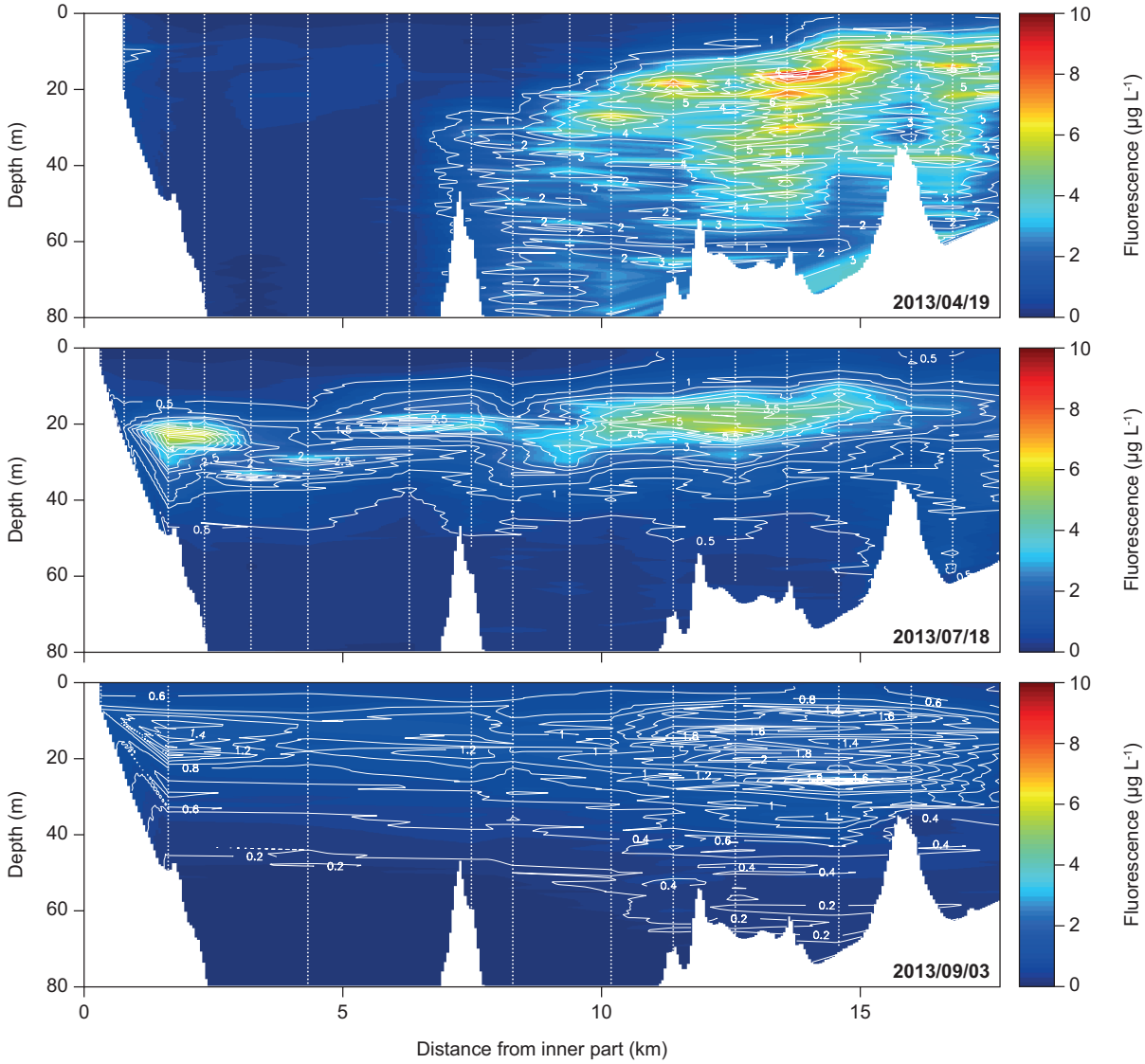
Depth (m)
Fluorescence (μg L-1)
2013/04/19
2013/07/18
2013/09/03
Distance from inner part (km)

Fig. A3

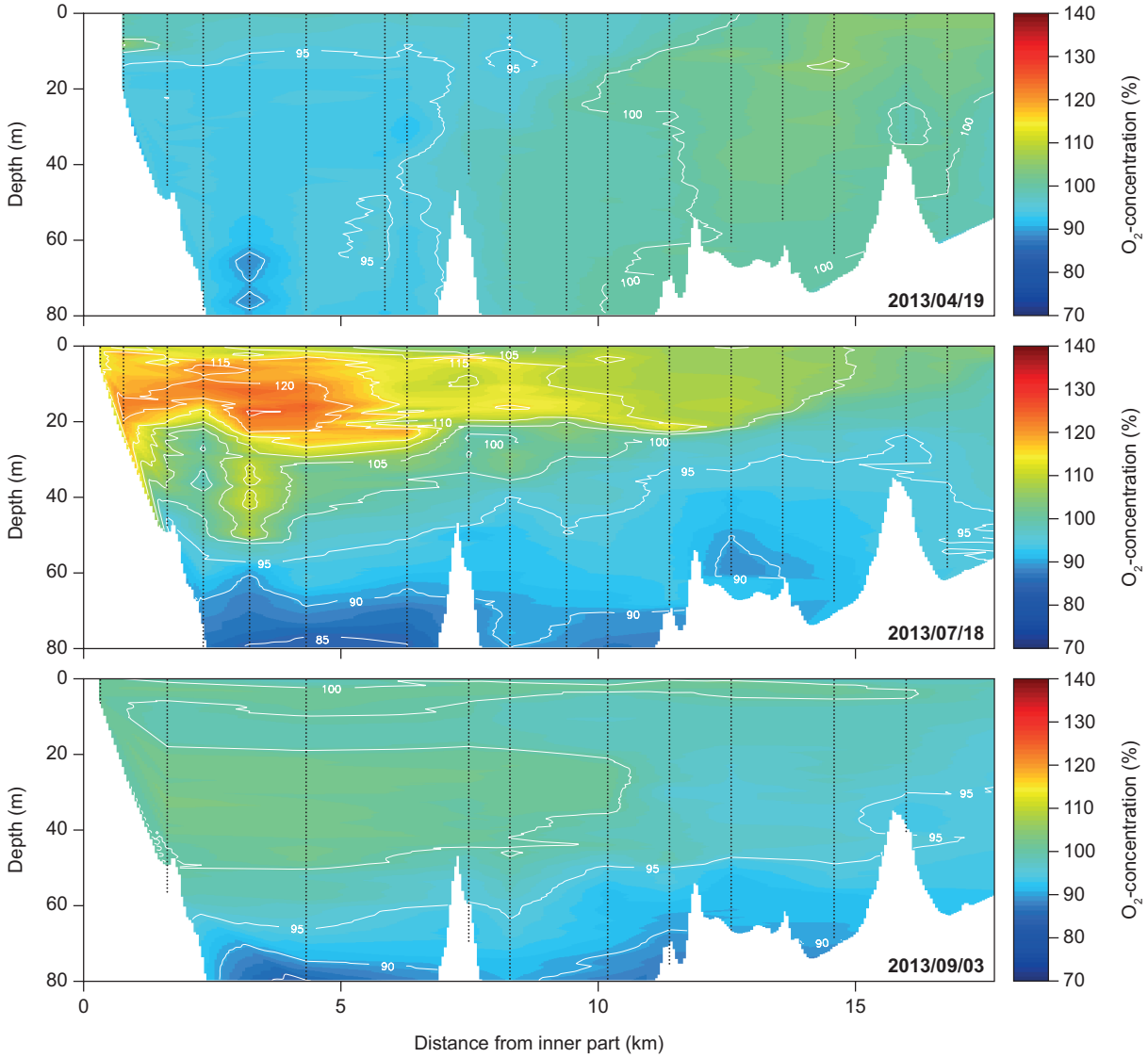
Depth (m)
0
20
40
60
80
2013/04/19
2013/07/18
2013/09/03
O2-concentration (%)
140
130
120
110
100
90
80
70
0
5
10
15
Distance from inner part (km)